Hindawi Publishing Corporation
Journal of Chemistry
Volume 2016, Article ID 6509212, 9 pages
http://dx.doi.org/10.1155/2016/6509212

Research Article

Fucofuroeckol-A from *Eisenia bicyclis* Inhibits Inflammation in Lipopolysaccharide-Induced Mouse Macrophages via Downregulation of the MAPK/NF-κB Signaling Pathway

Sang-Hoon Lee,[1] Sung-Hwan Eom,[1] Na-Young Yoon,[2] Moon-Moo Kim,[3] Yong-Xin Li,[4] Sang Keun Ha,[1] and Se-Kwon Kim[4,5]

[1]*Korea Food Research Institute, Baekhyun-dong, Seongnam, Gyeonggi 13539, Republic of Korea*
[2]*Food and Safety Research Center, National Fisheries Research & Development, Busan 46083, Republic of Korea*
[3]*Department of Chemistry, Dong-Eui University, Busan 47340, Republic of Korea*
[4]*Marine Bioprocess Research Center, Pukyong National University, Busan 48513, Republic of Korea*
[5]*Department of Specialized Graduate School Science and Technology Convergence, Pukyong National University, Busan 48547, Republic of Korea*

Correspondence should be addressed to Se-Kwon Kim; sknkim@pknu.ac.kr

Received 28 March 2016; Revised 16 May 2016; Accepted 25 May 2016

Academic Editor: Patricia Valentao

Fucofuroeckol-A (FF) isolated from an edible perennial brown seaweed *Eisenia bicyclis* was shown to be potent anti-inflammatory agents. FF suppressed the production of nitric oxide (NO) and prostaglandin E_2 (PGE_2) and the expression of inducible nitric oxide synthase and cyclooxygenase-2 dose dependently in lipopolysaccharide- (LPS-) induced RAW 264.7 mouse macrophages. An enzyme-linked immunosorbent assay and cytometric bead array assay demonstrated that FF significantly reduced the production of proinflammatory cytokines, such as interleukin-6 and tumor necrosis factor-α, and that of the monocyte chemoattractant protein-1. Moreover, FF reduced the activation of nuclear factor κB (NF-κB) and mitogen-activated protein kinases (MAPKs). These results strongly suggest that the inhibitory effects of fucofuroeckol-A from *E. bicyclis* on LPS-induced NO and PGE_2 production might be due to the suppression of the NF-κB and MAPK signaling pathway.

1. Introduction

Eisenia bicyclis is an edible perennial brown alga belonging to the family Lessoniaceae. This species is distributed widely in Korea and Japan. It is particularly abundant on Ulleung Island in South Korea. It is frequently used as a food-stuff, along with *Ecklonia cava* and *Ecklonia stolonifera*. The bioactive components of *E. bicyclis*, such as phlorotannins, polysaccharides, fucoxanthin, pyropheophytins, tripeptides, and oxylipin, have been investigated, and numerous biological activities, including anti-inflammatory, antitumor, antidiabetic, antioxidative, and neuroprotective, have been identified [1–6].

Inflammation is a complex process, which is regulated by a cascade of various proinflammatory cytokines, growth factors, nitric oxide (NO), and prostaglandins that are produced by activated macrophages [7]. One of the most significant mechanisms of inflammation is the production of NO by inducible nitric oxide synthase (iNOS) [8]. NO is a key vertebrate biological messenger, with important regulatory roles in various biological process [9]. Increased NO mediates various biological functions, such as nonspecific host defense, antimicrobial defense, and antitumor activities, as well as pathological processes, which include the pathogenesis of septic shock and organ destruction in some inflammatory and autoimmune diseases [10]. NO produced from the oxidation of the terminal guanidine of L-arginine by endothelial NOS is a potent powerful vasodilator. It possesses various vasoprotective effects, such as the inhibition of platelet aggregation, suppression of adhesion of leukocytes or monocytes on endothelial surfaces, and inhibition of proliferation and migration of vascular smooth muscle cells [11].

However, excessive NO production results in inflammatory tissue injury and several diseases [11, 12]. Transcriptionally expressed iNOS is responsible for excessive production of NO in activated macrophages. Therefore, the inhibition of NO overexpression by blocking iNOS expression offers a promising strategy for the treatment of a range of inflammatory disorders. Macrophages are white blood cells within tissues that play an important role in inflammatory processes and host defenses [13]. Proinflammatory stimuli, such as bacterial lipopolysaccharides (LPS), interferon-γ (IFN-γ), proinflammatory cytokines, and tumor necrosis factor-α (TNF-α), induce the activation of macrophages, resulting in the production of inflammatory mediators [14, 15]. LPS is a major component of the outer membrane of gram-negative bacteria and consists of lipids and polysaccharides. LPS acts as a prototypical endotoxin when gram-negative bacteria multiply in the host. It induces strong cellular immune responses, such as TNF-α, interleukin-6 (IL-6), prostaglandin E_2 (PGE_2), and NO, in animals in response to inflammation [16].

In this study, we investigated the inhibitory effects of fucofuroeckol-A (FF) derived from *E. bicyclis* on endotoxin-stimulated proinflammatory enzymes, such as iNOS and cyclooxygenase-2 (COX-2), which reduce iNOS-derived NO and COX-2-derived PGE_2 production in RAW 264.7 cells. Furthermore, we studied various intracellular signaling pathways, including nuclear factor κB (NF-κB) activity, inflammatory cytokine expression, and mitogen-activated protein kinases (MAPKs), which are thought to be activated in response to LPS stimulation of RAW 264.7 cells.

2. Materials and Methods

2.1. Materials and Chemicals. *E. bicyclis* was purchased from Ullengdomall (Ulleung Island, Korea) in March 2008. The samples were ground with grinder, and the alga powders were stored in a freezer at −20°C until use. LPS, 3-(4,5-dimethylthiazol-2-yl)-2,5-diphenyltetrazolium bromide (MTT), and dexamethasone (Dexa) were obtained from Sigma Co. (MO, USA). Specific antibodies against iNOS, COX-2, p65, I-κB, extracellular signal-regulated kinase (ERK), c-Jun N-terminal kinase (JNK), p38, phosphorylated p-ERK, p-p38, p-JNK, and p-I-κBα were purchased from Santa Cruz Biotechnology (CA, USA). All enzyme-linked immunosorbent assay (ELISA) kits for cytokines were purchased from Amersham Pharmacia Biosciences (NJ, USA), and a mouse inflammation cytometric bead array (CBA) kit was purchased from BD Biosciences (CA, USA). Sephadex LH-20, LiChroprep RP-18, and 0.25 mm precoated silica gel plates (Kieselgel 60 F_{254}) for chromatography were purchased from Merck (Darmstadt, Germany). All the solvents and chemicals used in this study were of reagent grade from commercial sources.

2.2. Extraction and Isolation. Lyophilized powder of *E. bicyclis* (3.8 kg) was extracted three times with 10 liters of hot methanol (MeOH). The MeOH extract (624.3 g) was partitioned with organic solvents to yield dichloromethane (CH_2Cl_2) (170.5 g), ethyl acetate (EtOAc) (90.4 g), and *n*-butanol (BuOH) (100.8 g) fractions, in addition to a water (H_2O) layer (262.6 g). The EtOAc fraction was subjected to chromatographic separation using Sephadex LH-20 (100% methanol elution) and LiChroprep RP-18 (Merck; 20–100% methanol gradient elution) columns. The subfractions showing the greatest activities were further purified using Sephadex LH-20 and LiChroprep RP-18 with methanol. Thin layer chromatography (TLC) was conducted on precoated Merck Kieselgel 60 F_{254} plates (20 × 20 cm, 0.25 mm), using 50% H_2SO_4 as a spray reagent [17]. To characterize the isolated compound, the ^{1}H- and ^{13}C-nuclear magnetic resonance (NMR) spectra were determined using a JEOL JNM-ECP 400 spectrometer (Tokyo, Japan; 400 MHz for ^{1}H-NMR and 100 MHz for ^{13}C-NMR) in dimethyl sulfoxide (DMSO)d_6. The chemical shifts were referenced to residual solvent peaks (2.49 ppm for ^{1}H-NMR and 39.50 ppm for ^{13}C-NMR).

2.3. Cell Culture. A RAW 264.7 mouse macrophage cell line was maintained in Dulbecco's Modified Eagle's Medium (DMEM) (GIBCO, New York, USA), supplemented with 100 μg/mL of penicillin-streptomycin and 10% fetal bovine serum at 37°C in a humidified incubator under 5% CO_2. Confluent cultures were washed twice with phosphate buffered saline (PBS) and then collected with a scraper. The collected cells were resuspended in DMEM and seeded in a cell culture dish or well plates [6].

2.4. Cell Viability (MTT) Assay. The cytotoxicity levels of the RAW 264.7 macrophages treated with FF were measured using the MTT method as described by Hansen et al. [18], with slight modifications. The RAW 264.7 cells were cultured in 96-well plates at a density of 1×10^5 cells/well. After 24 h, the cells were washed with fresh medium and treated with various concentrations of samples. After incubation for 24 h, the cells were washed two times with PBS, and 100 μL of MTT solution (1 mg/mL) was added to each well for 3 h. After removing the medium, 100 μL of DMSO was added to solubilize the formed formazan salt. The amount of formazan salt was determined by measuring the optical density (OD) at 540 nm using a UV microplate reader (Tecan Austria GmbH, Groedig, Austria). The data were expressed as the means of at least three independent experiments. Each value was expressed as the mean ± SD of triplicate experiments.

2.5. Nitrite Assay. To examine the inhibitory effects of FF on LPS-stimulated NO production in the RAW 264.7 cells, we measured nitrite released into the culture medium using Griess reagent. The RAW 264.7 cells were treated with various concentrations of FF (1, 10, 50, and 100 μM) for 1 h before the addition of LPS (1 μg/mL). The concentrations of NO in culture supernatants were determined by measuring nitrite, a major stable product of NO, using Griess reagent (1% sulfanilic acid and 0.2 mM N-[1-naphthyl] ethylenediamine-HCl in 2.5% H_3PO_4) [19]. The cells were grown at a density of 1×10^5 cells/well and treated with different concentrations of FF for 1 h before incubation with LPS (1 μg/mL) for 24 h. Then, 100 μL of each culture supernatant was mixed with the same volume of Griess reagent. The nitrite levels of each

sample were determined colorimetrically at 540 nm using an ELISA microplate reader (Tecan Austria GmbH). The standard curve of nitrite concentrations was calculated with sodium nitrite.

2.6. Determination of TNF-α and IL-1β Using an ELISA. The levels of TNF-α and IL-1β were determined using Biotrak™ ELISA kits (Amersham Pharmacia Biosciences) according to the manufacturer's instructions [20]. Briefly, the cells were grown at a density of 1×10^5 cells/well and treated with different concentrations of the sample for 1 h before incubation with LPS (1 μg/mL) for the indicated times. Following incubation, 50 μL of medium was added to wells of antibody-coated 96-well plates. Then, 50 μL of biotinylated antibody reagent was added and incubated for 3 h at room temperature (RT). The reaction mixture was removed from each well and washed four times with washing buffer. Subsequently, 100 μL of streptavidin conjugated to horseradish peroxidase was added and incubated for 30 min at RT. After the same washing step as above, 100 μL of 3,3′,5,5′-tetramethylbenzidine (TMB) substrate solution was added and incubated for 30 min at RT. After adding 50 μL of stop solution, the optical density was measured at 450 nm using an ELISA microplate reader (Tecan Austria GmbH).

2.7. Determination of Prostaglandin E_2 (PGE_2) Using a PGE_2 Direct Assay. To assess whether FF could inhibit the production of LPS-induced PGE_2 in RAW 264.7, the cells were pretreated with FF for 1 h before incubation with LPS (1 μg/mL) for 24 h. After incubation for 24 h, the cell culture medium was harvested, and the production of PGE_2 was measured using an ELISA. The levels of PGE_2 were determined using Biotrak™ direct assay kits (Amersham Pharmacia Biosciences, NJ, USA) according to the manufacturer's instruction [20]. Briefly, cells were grown at a density of 1×10^5 cells/well and treated with different concentrations of FF for 1 h before incubation with LPS (1 μg/mL) for 24 h. Following incubation, 50 μL of medium was added to wells of antibody-coated 96-well plates. Then, 50 μL of mouse anti-PGE_2 and 50 μL of diluted conjugate were added and incubated for 1 h at RT on well plate shaker. The reaction mixture was removed from each well and washed four times with washing buffer. Subsequently, 150 μL of TMB enzyme substrate were added into each well and incubated for 30 min at RT on microplate shaker. After adding 100 μL of stop solution, the OD was measured at 450 nm using an ELISA microplate reader (Tecan Austria GmbH).

2.8. Determination of IL-6 and Monocyte Chemotactic Protein (MCP-1) Using a CBA. The levels of IL-6 and MCP-1 were determined using a BD™ CBA Mouse Inflammation kit (BD Biosciences, San Diego, USA) with flow cytometry according to the manufacturer's instructions [21]. Briefly, the cells were grown at a density of 1×10^5 cells/well and treated with different concentrations of FF for 1 h before incubation with LPS (1 μg/mL) for 24 h. Following incubation, 50 μL of medium and 50 μL of capture bead mixture were added to a 5 mL tube and treated with 50 μL of phycoerythrin (PE) detection reagent. Following incubation for 2 h, the reaction mixture was washed with 1 mL of wash buffer and centrifuged for 5 min at 5,000 rpm. Finally, the bead-captured cells were resuspended with 300 μL of wash buffer and analyzed by flow cytometry (BD Biosciences, San Diego), calibrated with a cytometer setup bead procedure. The results were analyzed using BD™ CBA software (BD Biosciences).

2.9. Reverse Transcriptase-Polymerase Chain Reaction (RT-PCR). To confirm whether the inhibition of NO and PGE_2 production was due to a decreased level of iNOS and COX-2, the effects of FF on the level of iNOS and COX-2 mRNA and protein were determined by RT-PCR and Western blot analysis, respectively. The RAW 264.7 cells were treated with different concentrations of FF for 1 h before incubation with LPS (1 μg/mL) for 12 h. The cells were harvested and washed twice with PBS. The total RNA was isolated using TRIzol reagent (Invitrogen, CA, USA). Chloroform was added to the cell lysate and centrifuged at 13,000 ×g for 12 min, and the supernatant was collected. The same volume of isopropanol was added, and the RNA pellet was collected following centrifugation. After washing with 70% ethanol, extracted RNA was dissolved in diethylpyrocarbonate-treated RNase-free water and incubated for 10 min at 60°C. The RNA concentration was quantified by measuring the OD at 260 nm using a microplate reader (Tecan Austria GmbH). Then, 1 μg of RNA obtained from the cells was reverse-transcribed using M-MLV reverse transcriptase (Promega, Madison, WI) at 42°C for 45 min to produce cDNAs. RT-generated cDNA was used as a template to amplify iNOS, COX-2, IL-1β, TNF-α, and glyceraldehyde-3-phosphate dehydrogenase (GAPDH) genes in a PCR mixture containing dNTPs and taq DNA polymerase (Promega). PCR was performed using a Whatman thermocycler (Biometra, Kent, UK) with selective upstream and downstream primers for mouse iNOS (5′-ATGTCCGAAGCAAACATCAC-3′ and 5′-TAATGTCCAGGAAGTAGGTG-3′), COX-2 (5′-CAGCAAATCCTTGCTGTTCC-3′ and 5′-TGGGCAAAGAATGCAAACATC-3′), IL-1β(5′-ATGGCAACTGTTCCTGAACTCAACT-3′ and 5′-TTTCCTTTCTTAGATATGGACAGGAC-3′), IL-6 (5′-AGTTGCCTTCTTGGGACTGA-3′ and 5′-CAGAATTGCCATTGCACAAC-3′), TNF-α (5′-ATGAGCACAGAAAGCATGATC-3′ and 5′-TACAGGCTTGTCACTCGAATT-3′), and GAPDH (5′-TGAAGGTCGGTGTGAACGGATTTGGC-3′ and 5′-CATGTAGGCCATGAGGTCCACCAC-3′) [22–24]. The amplified DNA was analyzed by 2% agarose gel electrophoresis and visualized by ethidium bromide staining. GAPDH was used as an internal control for sample loading and checking mRNA integrity.

2.10. Western Blot. We investigated the effect of FF on LPS-induced p-NF-κB p65 nuclear translocation as measured by Western blot analysis. Furthermore, to determine whether the inhibition of p-NF-κB p65 DNA binding by FF was related to p-I-κBα, cytoplasmic levels of p-I-κBα were examined by Western blot analysis [25]. The RAW 264.7 cells were treated with different concentrations of FF for 1 h before incubation with LPS (1 μg/mL) for 24 h. To obtain the cytoplasmic protein, the cells were harvested and washed twice with PBS. The collected cells were resuspended with lysis buffer (pH 7.5,

50 mM Tris-HCl, 0.4% Nonidet P-40, 120 mM NaCl, 1.5 mM $MgCl_2$, 2 mM phenylmethylsulfonyl fluoride, 80 μg/mL of leupeptin, 3 mM NaF, and 1 mM DTT) and incubated at 4°C for 20 min. Cell lysates were centrifuged at 12,000 rpm for 10 min, and the protein concentrations of the supernatants were determined with the Lowry method, using bovine serum albumin as a standard. To separate the nuclear extracts, CelLytic™ NuCLEAR™ extraction kit (Sigma-Aldrich Co.) was used according to the manufacturer's instructions [26]. The proteins (20–40 μg) were diluted in 5x protein loading buffer (10% SDS, 100 mM each dithiothreitol, glycerol, bromophenol blue, and tris-HCl) and denatured at 100°C for 10 min. Protein extracts were separated on 10 or 12% SDS-polyacrylamide gels and transferred to a Hybond ECL nitrocellulose membrane (Amersham Biosciences). Transferred protein blots were blocked with 1% bovine serum albumin in Tris-buffered saline containing 0.1% Tween 20 for 1 h at RT. The membrane was washed three times with Tris-buffered saline containing 0.1% Tween 20 and incubated with primary antibodies (1 : 500 dilution) for 1 h at RT. After washing three times with Tris-buffered saline containing 0.1% Tween 20, the membrane was incubated with corresponding horseradish peroxidase-conjugated secondary antibody (1 : 5000 dilution) for 1 h at RT. After washing the membrane four times with Tris-buffered saline containing 0.1% Tween 20, the membrane was developed with a chemiluminescence reagent (ECL reagent; Amersham Biosciences). Blot bands were visualized using an LAS3000 Luminescent image analyzer (Fujifilm Life Science, Tokyo, Japan).

2.11. Electrophoretic Mobility Shift Assay (EMSA). The RAW 264.7 cells were pretreated with FF for 1 h before stimulation with LPS (1 μg/mL) for another 15 min. An EMSA for NF-κB was performed by employing a Lightshift™ Chemiluminescent EMSA kit (Pierce, IL, USA) according to the manufacturer's protocol [27]. Nuclear extracts were prepared using a CelLytic™ NuCLEAR™ extraction kit (Sigma-Aldrich Co.) according to the manufacturer's instructions. Briefly, DNA was biotin-labeled using a Biotin 3′ End DNA Labeling kit (Pierce, IL, USA). In 50 μL of reaction buffer, 10 pmol of double-stranded NF-κB oligonucleotide (5′-AGTTGAGGGGACTTTCCCAGGC-3′; 3′-TCAACTCCCCTGAAAGGGTCCG-5′) was incubated in 10 μL of 5x TdT buffer, 5 μL of unlabeled control oligo (100 nM), 5 μL of biotin-11-dUTP (0.5 μM), 5 μL of diluted TdT (2 U/μL), and 25 μL of ultrapure water at 37°C for 30 min. The reaction was stopped with 2.5 μL of 0.2 M EDTA and treated with 50 μL of chloroform : isoamyl alcohol (24 : 1) for DNA extraction. Following centrifugation at 15,000 ×g for 2 min, the top aqueous phase containing the labeled DNA was used for further binding reactions. The binding reactions contained 3–5 μg of nuclear extract protein, buffer (10 mM Tris, pH 7.5, 50 mM KCl, 5 mM $MgCl_2$, 1 mM dithiothreitol, 0.05% NP-40, and 2.5% glycerol), 50 ng of poly(dI-dC), and 30 fM of biotin end-labeled DNA. The binding reactions were incubated for 20 min at RT in a final volume of 20 μL. The reaction mixture was subjected to gel electrophoresis on 5% polyacrylamide gel and transferred to a nylon membrane (Biodyne® Precut Nylon Membranes, IL, USA). DNA was cross-linked to the membrane using a UV cross-linker (Bio-Link, Vilber Lourmat, France) at 120 mJ/cm^2, and the spectral peak was detected at 312 nm using an LAS3000 image analyzer (Fujifilm Life Science).

2.12. NF-κB/p65 Nuclear Localization Imaging Using Confocal Laser Scanning Microscopy. The nuclear localization of NF-κB was detected by indirect immunofluorescence assays using confocal microscopy [28]. The RAW 264.7 cells were cultured directly on glass coverslips in 24-well plates for 24 h and treated with different concentrations of FF for 1 h before incubation with LPS (1 μg/mL) for 15 min. After incubation with LPS, the cells were fixed with 4% paraformaldehyde in PBS, permeabilized with 0.2% Triton X-100 in PBS, and blocked with 1.5% normal donkey serum. Polyclonal antibodies against NF-κB (1 μg/well) were applied for 1 h, followed by 1 h of incubation with fluorescein isothiocyanate- (FITC-) conjugated donkey anti-rabbit IgG (Jackson ImmunoResearch Laboratories, Inc., West Grove, PA). After washing with PBS, the coverslips were mounted in Fluoromount-G (Southern Biotechnology Associates Inc., Birmingham, AL, USA), and the fluorescence was visualized using a Zeiss LSM 510 confocal laser scanning microscope (Carl Zeiss, Jena, Germany).

2.13. Statistical Analysis. All the data are presented as means ± SD. The mean values were calculated based on the data taken from at least three independent experiments conducted on separate days using freshly prepared reagents. Statistical significance was accepted at a value of $P < 0.05$.

3. Results

3.1. Structural Elucidation of FF. The inhibitory effects on NO production were significantly correlated with the total phenolic compounds [29]. The EtOAc-soluble fraction from *E. bicyclis* showed the highest total phenolic contents [17]. In addition, it showed the highest inhibitory effects on NO production among organic solvent-soluble fraction (data not shown). FF (250.3 mg) was isolated from the ethyl acetate extract (90.4 g) of the marine edible perennial brown alga *E. bicyclis*. The chemical structure was elucidated by a comprehensive spectral analysis of ^{1}H and a comparison of ^{13}C, ^{1}D NMR data to data published previously [17, 30]. The structure of FF was assigned as illustrated in Figure 1(a).

FF: Pale brown powder, $C_{22}H_{14}O_{11}$. ^{1}H NMR (DMSO-d_6, 400 MHz) δ 10.05 (1H, s, 14-OH), 9.88 (1H, s, 4-OH), 9.76 (1H, s, 10-OH), 9.44 (1H, s, 2-OH), 9.18 (2H, s, 3′, 5′-OH), 8.22 (1H, s, 8-OH), 6.71 (1H, s, H-13), 6.47 (1H, d, J = 1.1 Hz, H-11), 6.29 (1H, s, H-3), 6.25 (1H, d, J = 1.5 Hz, H-9), 5.83 (1H, s, H-4′), 5.76 (2H, d, J = 1.5 Hz, H-2′, 6′); ^{13}C NMR (DMSO-d_6, 100 MHz) δ 160.7 (C-1′), 158.8 (C-3′, 5′), 158.3 (C-11a), 157.6 (C-10), 150.5 (C-12a), 150.2 (C-8), 146.9 (C-2), 144.4 (C-14), 142.0 (C-4), 136.8 (C-15a), 133.6 (C-5a), 126.1 (C-14a), 122.6 (C-4a), 122.4 (C-1), 103.1 (C-6), 102.4 (C-7), 98.2 (C-3), 98.0 (C-9), 96.3 (C-4′), 94.6 (C-13), 93.7 (C-2′, 6′), 90.5 (C-11).

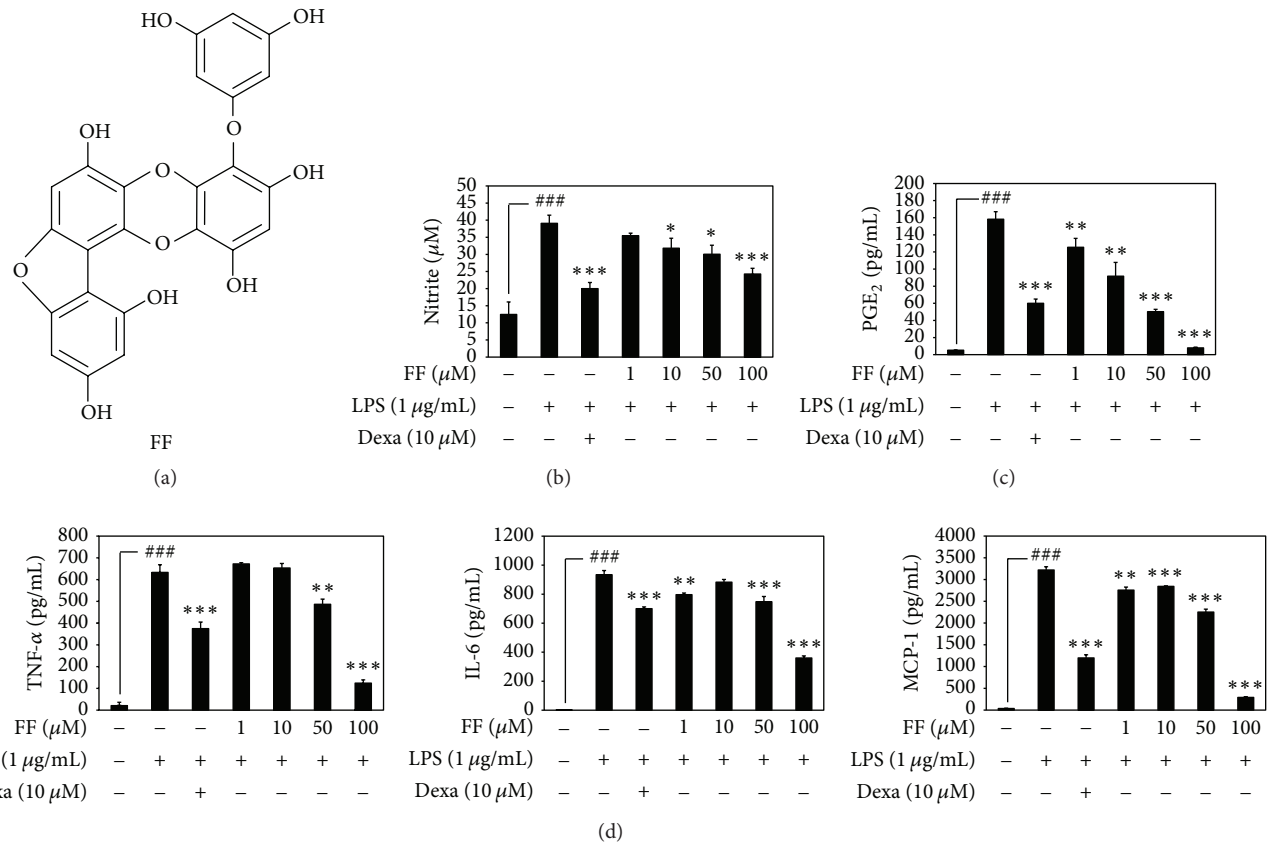

Figure 1: Elucidation of the structure of FF from the edible perennial brown alga *Eisenia bicyclis* (a). Effect of FF on LPS-induced NO production in RAW 264.7 macrophages (b). Effect of FF on LPS-induced production of PGE_2 in RAW 264.7 macrophages (c). Effect of FF on LPS-induced production of proinflammatory cytokines in RAW 264.7 macrophages (d). The cells were grown at a density of 1×10^5 cells/well and treated with different concentrations of FF for 1 h before incubation with LPS (1 μg/mL) for 24 h. Each value was expressed as the mean ± SD of triplicate experiments. $^{*}P < 0.05$, $^{**}P < 0.01$, and $^{***}P < 0.001$ as compared with LPS-treated cells (1 μg/mL). $^{\#\#\#}P < 0.001$ as compared with LPS nontreated cells.

3.2. Effects of FF on NO Production in the LPS-Stimulated RAW 264.7 Cell Line. The viabilities of the FF were assessed in LPS-stimulated RAW 264.7 cell line. FF exerted no cytotoxic effects even at the highest concentration of 100 μM (data not shown). Pretreatment with the different doses of FF led to a significant reduction in the formation of NO in a dose-dependent manner, as measured in the supernatants 24 h following LPS stimulation (Figure 1(b)). According to the NO detection assay, NO was significantly increased (3.13 times that of the basal level) after 24 h of LPS stimulation, and the FF treatment inhibited this increase, with relative NO production of 62.1% and 53.8%, respectively, compared to that of a nontreated control.

3.3. Effects of FF on the Production of PGE_2 in the LPS-Stimulated RAW 264.7 Cell Line. Pretreatment of the LPS-stimulated cells with FF (1, 10, 50, and 100 μM) resulted in a significant dose-dependent reduction in the production of PGE_2 (Figure 1(c)). In the present study, 10 μM of ketoprofen showed strong inhibitory activity against the production of PGE_2 (inhibition of 97.6%) (not shown). As shown in Figure 1(c), pretreatment with FF significantly and dose dependently suppressed the expression of LPS-stimulated proinflammatory mediators. At a concentration of 100 μM, FF strongly suppressed the production of PGE_2, with 4.3% of relative production compared to that of a control.

3.4. Effects of FF on the Production of TNF-α, IL-6, and MCP-1 in the LPS-Stimulated RAW 264.7 Cell Line. As shown in Figure 1(d), TNF-α and IL-6 levels increased significantly in the culture media of the LPS-stimulated RAW 264.7 cells, and these increases were significantly decreased in a concentration-dependent manner by the treatment with FF. The results indicate that FF negatively regulated the accumulation of proinflammatory cytokines at the transcriptional level. Furthermore, MCP-1 levels increased significantly in the culture media of the LPS-stimulated RAW 264.7 cells, and the treatment with FF remarkably decreased these levels in a dose-dependent manner (Figure 1(d)). Therefore, MCP-1 could be a potential marker to assess inflammation. The results of the present study indicated that FF reduced the production of MCP-1 by suppressing inflammatory cytokines and reducing the inflammation.

3.5. Effects of FF on the Expression of iNOS and COX-2 in the LPS-Stimulated RAW 264.7 Cells. The expression of

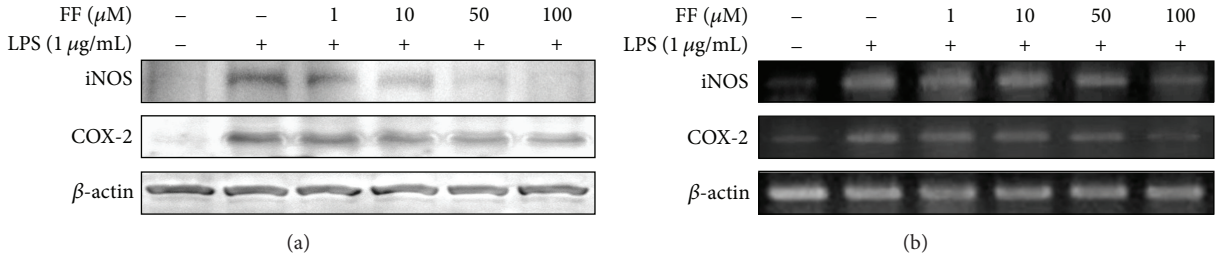

Figure 2: Effect of FF on LPS-induced protein (a) and mRNA (b) expression of iNOS and COX-2 in RAW 264.7 macrophages. The cells were grown at 5×10^5 cells/well and treated with various concentrations of FF for 1 h before LPS (1 μg/mL) treatment. After incubation for 12 h (RT-PCR) and 24 h (Western blot), cell lysates were collected and subjected to Western blot and RT-PCR analysis.

iNOS and COX-2 proteins was barely detectable in the unstimulated in RAW 264.7 cell line, whereas their expression markedly increased after 24 h of the LPS (1 μg/mL) treatment. FF significantly attenuated iNOS and COX-2 protein expression in the LPS-stimulated RAW 264.7 cells (Figure 2(a)). The effects of FF on iNOS and COX-2 mRNA expression were also evaluated. RT-PCR analysis showed that the expression of iNOS and COX-2 mRNA was correlated with their protein levels (Figure 2(b)). These results indicate that LPS exposure increased the expression of iNOS and COX-2 mRNA and proteins and that the treatment with FF significantly suppressed the induction of LPS-stimulated mediators through transcriptional inhibition.

3.6. Effects of FF on LPS-Induced Nuclear Translocation of NF-κB and LPS-Induced p-I-κBα Levels. As shown in Figure 3(a), the regulation of p-NF-κB p65 was translocated to the nucleus after the LPS treatment for 15 min. The p-NF-κB p65 protein was decreased in the nucleus of cells exposed to LPS following the FF treatment, verifying that this phlorotannin inhibited the nuclear translocation of the p-NF-κB p65 protein. The pretreatment of the RAW 264.7 cells with FF was blocked LPS-induced p-I-κBα. The decrease in the p-I-κBα protein in the RAW 264.7 cells provided strong evidence that FF inhibited the activation of NF-κB.

To understand the influence of FF and on NF-κB nuclear translocation, immunofluorescence analysis was performed to assess the influence of FF on the nuclear translocation of NF-κB in the RAW 264.7 cells (Figure 3(b)). After fixation, the cells were stained with antibody and observed at 400x magnification. Confocal images revealed that NF-κB was sequestered in the cytoplasmic compartment in the absence of LPS stimulation but that it accumulated in the RAW 264.7 cells after LPS stimulation. Pretreatment of the cells with FF completely abolished the LPS-induced translocation of NF-κB. The results showed that FF inhibited the translocation of NF-κB. To further characterize the inhibitory effects of FF on the expression of iNOS and COX-2, NF-κB DNA-binding activity was determined by an EMSA (Figure 3(c)). The LPS treatment significantly increased the DNA-binding activity of NF-κB. Although FF did not inhibit the NF-κB DNA-binding activity, it exerted an inhibitory effect on the translocation of NF-κB, suggesting that it may be responsible for the suppression of NO, PGE_2, and proinflammatory cytokines in the RAW 264.7 macrophages.

3.7. Effects of FF on the Phosphorylation of MAPKs in the LPS-Stimulated RAW 264.7 Cell Line. We confirmed that ERK1/2, JNK, and p38 kinase were phosphorylated by stimulation with LPS. As shown in Figure 4, FF (100 μg/mL) remarkably inhibited JNK and p38 kinase activation, whereas neither treatment affected the phosphorylation of ERK1/2. These results suggest that phosphorylation of JNK and p38 is involved in the inhibitory effect of FF on LPS-induced iNOS and COX-2 expression in RAW 264.7 cells.

4. Discussion

Nonsteroidal anti-inflammatory drugs, such as ketoprofen, have been shown to have therapeutic potential in the treatment of inflammatory disease via the inhibition of COX, which is responsible for the biosynthesis of prostaglandins [31]. However, ketoprofen has side effects, such as gastrointestinal ulcers and kidney damage, due to concomitant inhibition of COX-1 [32]. Therefore, the search for nontoxic inflammatory drugs from marine-derived bioresources is of great interest to researchers. Recently, marine-derived plant remedies have become increasingly popular and are widely used for healthcare and inflammation prevention. Several researchers have reported the anti-inflammatory effects of phlorotannins (marine-derived polyphenols) from edible brown seaweed such as eckol, phlorofucofuroeckols, dieckol, phloroglucinol, and bieckols [5, 33]. However, limited information is available on the anti-inflammatory effects of FF among phlorotannins. Particularly, there have been few reports of its biological activities as antioxidant activity [34] and anticancer activity [35]. Therefore, we tried to identify the anti-inflammatory effect of FF in RAW 264.7 cells induced by LPS and we found that FF from edible seaweed *E. bicyclis* decreased NO and PGE_2 overproduction in LPS-activated RAW 264.7 macrophages. Therefore, it was necessary to elucidate the molecular mechanisms by which they function. In this present study, we found that FF attenuated the mRNA and protein expression of iNOS and COX-2. These results indicate that the actions of FF occur at the transcriptional level. We also evaluated the suppressive effects of FF on the production of proinflammatory cytokines, such as TNF-α and IL-6, and that of the proinflammatory chemokine, MCP-1. Our results indicate, for the first time, that the activity of the AP-1 transcription factor was significantly downregulated by FF in LPS-stimulated macrophage cells.

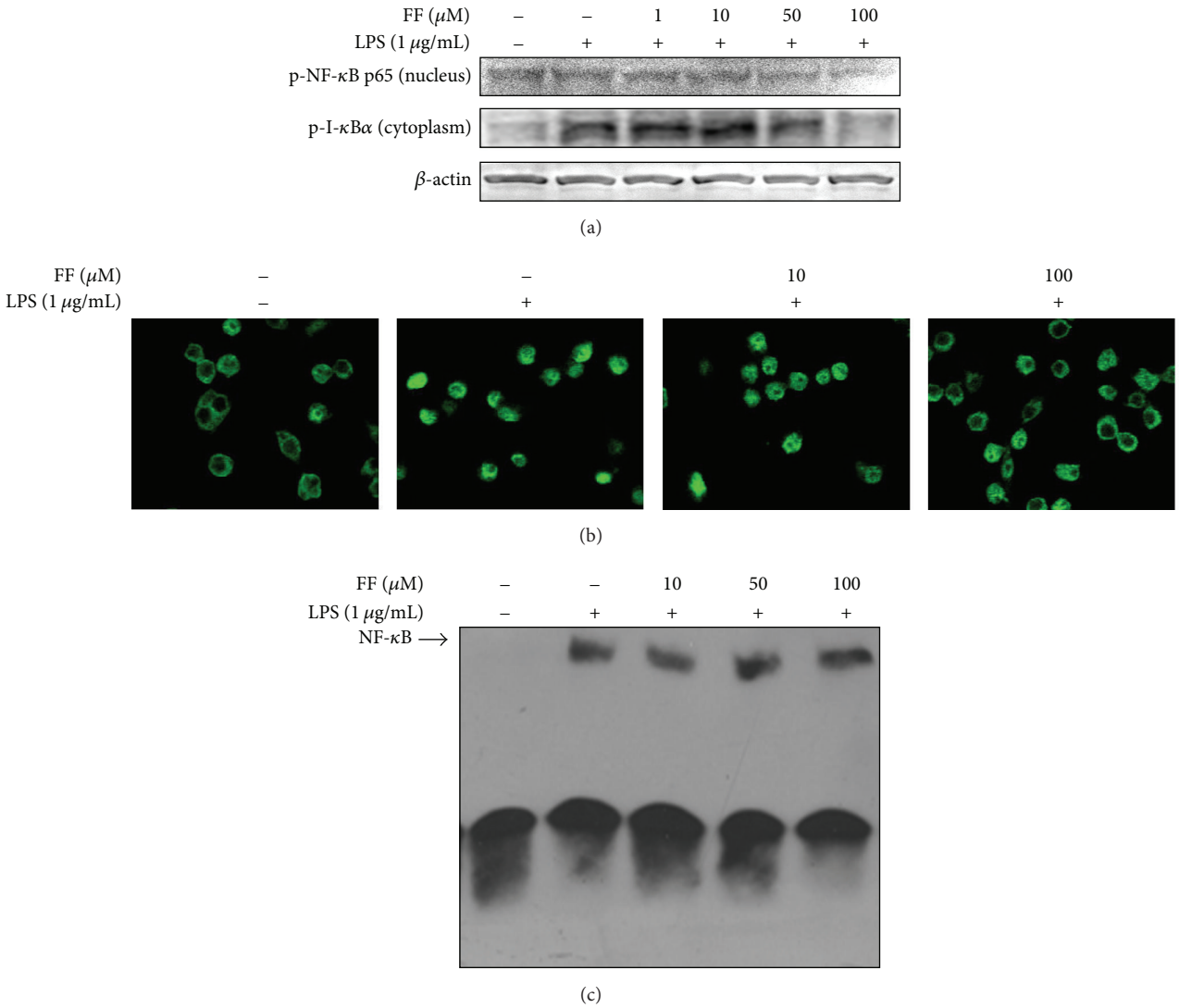

Figure 3: Effects of FF on NF-κB translocation and p-I-$\kappa B\alpha$ expression in LPS-induced RAW 264.7 macrophages. (a) Western blot analysis showing the effect of FF treatment on expression of p-p65 and p-I-$\kappa B\alpha$ in cytoplasmic and nuclear extracts. The cells were grown at 5×10^5 cells/well and treated with various concentrations FF for 1 h before LPS (1 μg/mL) treatment. After incubation for 24 h, cell lysates were collected and subjected to Western blots using antibodies specific for p-p65 and p-I-$\kappa B\alpha$. (b) The localization of the p-p65 protein in cells was determined with an antibody and an FITC-labeled anti-rabbit IgG antibody using confocal laser scanning microscopy. (c) p-p65-binding activities using an EMSA.

Furthermore, we examined the anti-inflammatory mechanisms of FF and found that they involved the inhibition of LPS-mediated activation of the NF-κB signaling pathway. FF inhibited the phosphorylation of I-$\kappa B\alpha$ and furthermore suppressed p-NF-κB p65 translocation to the nucleus. As the binding activity of NF-κB is known to regulate the expression of proinflammatory mediators, including cytokines and chemokines, we performed an EMSA to determine whether FF inhibited NF-κB activity. However, FF did not exhibit inhibitory activity against NF-κB DNA binding in the RAW 264.7 macrophages.

In addition, we investigated the effects of FF on the phosphorylation of ERK1/2, JNK, and p38 kinase in LPS-stimulated RAW 264.7 cells. Interestingly, the FF treatments decreased the phosphorylation of JNK and p38 kinase in response to LPS. However, we observed no significant FF-induced changes in the LPS-induced phosphorylation of ERK1/2. Hence, these results suggest that JNK and p38, but not ERK1/2, is involved in the inhibitory effect of FF on LPS-induced iNOS and COX-2 expression and NF-κB activation. Our results clearly indicate that FF show remarkable dose-dependent anti-inflammatory activities, without any cytotoxic effects, illustrating their strong potential as promising therapeutic candidates for inflammatory diseases.

5. Conclusions

We investigated the anti-inflammatory effects of FF from *E. bicyclis* on the production of NO and PGE_2 and on the expression of iNOS, COX-2, cytokines (TNF-α, IL-1β, and

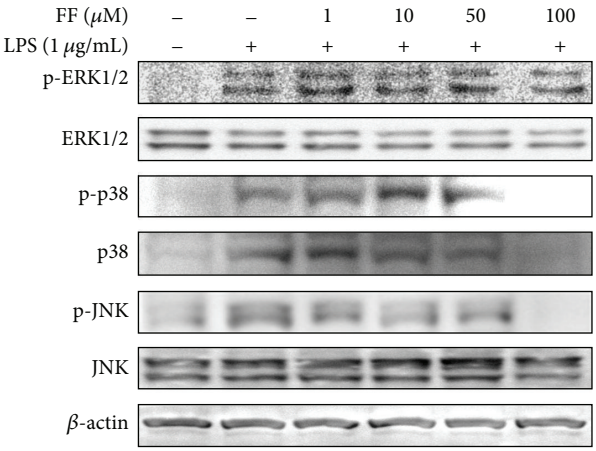

FIGURE 4: Effect of FF on LPS-induced protein expression of MAPKs in RAW 264.7 macrophages. The cells were grown at 5×10^5 cells/well and treated with various concentrations of FF 1 h before LPS (1 μg/mL) treatment. After incubation for 24 h, cell lysates were collected and subjected to Western blots.

IL-6), and chemokines (MCP-1). Our results clearly indicate that FF are effective inhibitors of LPS-induced cytokines and chemokines and the expression of iNOS and COX-2 and that they act by blocking the NF-κB and MAPK signaling pathways in RAW 264.7 cells. The present data also suggest that FF may be a valuable natural anti-inflammatory agent in the development of nutraceuticals and pharmaceuticals.

Competing Interests

The authors declare that there are no compteing interests regarding the publication of this paper.

Authors' Contributions

Sang-Hoon Lee and Sung-Hwan Eom equally contributed to this paper.

Acknowledgments

This research was supported by Bioindustry Technology Development Program, Ministry of Agriculture, Food and Rural Affairs (112136-4).

References

[1] B. R. Ahn, H. E. Moon, H. R. Kim, H. A. Jung, and J. S. Choi, "Neuroprotective effect of edible brown alga *Eisenia bicyclis* on amyloid beta peptide-induced toxicity in PC12 cells," *Archives of Pharmacal Research*, vol. 35, no. 11, pp. 1989–1998, 2012.

[2] A. H. Cahyana, Y. Shuto, and Y. Kinoshita, "Pyropheophytin a as an antioxidative substance from the marine alga, arame (*Eisenia bicyclis*)," *Bioscience, Biotechnology, and Biochemistry*, vol. 10, pp. 1533–1535, 1992.

[3] S. Ermakova, R. Men'shova, O. Vishchuk et al., "Water-soluble polysaccharides from the brown alga *Eisenia bicyclis*: structural characteristics and antitumor activity," *Algal Research*, vol. 2, no. 1, pp. 51–58, 2013.

[4] H. A. Jung, M. N. Islam, C. M. Lee et al., "Promising antidiabetic potential of fucoxanthin isolated from the edible brown algae *Eisenia bicyclis* and *Undaria pinnatifida*," *Fisheries Science*, vol. 78, no. 6, pp. 1321–1329, 2012.

[5] H. A. Jung, S. E. Jin, B. R. Ahn, C. M. Lee, and J. S. Choi, "Anti-inflammatory activity of edible brown alga *Eisenia bicyclis* and its constituents fucosterol and phlorotannins in LPS-stimulated RAW264.7 macrophages," *Food and Chemical Toxicology*, vol. 59, pp. 199–206, 2013.

[6] N. Y. Yoon, S.-H. Lee, I. Wijesekara, and S.-K. Kim, "In vitro and intracellular antioxidant activities of brown alga *Eisenia bicyclis*," *Fisheries and Aquatic Science*, vol. 14, no. 3, pp. 179–185, 2011.

[7] L. M. Coussens and Z. Werb, "Inflammation and cancer," *Nature*, vol. 420, no. 6917, pp. 860–867, 2002.

[8] A. K. Nussler and T. R. Billiar, "Inflammation, immunoregulation, and inducible nitric oxide synthase," *Journal of Leukocyte Biology*, vol. 54, no. 2, pp. 171–178, 1993.

[9] Q. W. Xie, H. J. Cho, J. Calaycay et al., "Cloning and characterization of inducible nitric oxide synthase from mouse macrophages," *Science*, vol. 256, no. 5054, pp. 225–228, 1992.

[10] A. Petros, D. Bennett, and P. Vallance, "Effect of nitric oxide synthase inhibitors on hypotension in patients with septic shock," *The Lancet*, vol. 338, no. 8782-8783, pp. 1557–1558, 1991.

[11] M. Ozaki, S. Kawashima, T. Yamashita et al., "Overexpression of endothelial nitric oxide synthase accelerates atherosclerotic lesion formation in apoE-deficient mice," *Journal of Clinical Investigation*, vol. 110, no. 3, pp. 331–340, 2002.

[12] Y. Vodovotz, M. S. Lucia, K. C. Flanders et al., "Inducible nitric oxide synthase in tangle-bearing neurons of patients with Alzheimer's disease," *The Journal of Experimental Medicine*, vol. 184, no. 4, pp. 1425–1433, 1996.

[13] N. Shibata and C. K. Glass, "Regulation of macrophage function in inflammation and atherosclerosis," *Journal of Lipid Research*, vol. 50, pp. S277–S281, 2009.

[14] F. Berenbaum, "Proinflammatory cytokines, prostaglandins, and the chondrocyte: mechanisms of intracellular activation," *Joint Bone Spine*, vol. 67, no. 6, pp. 561–564, 2000.

[15] G. Zhang and S. Ghosh, "Molecular mechanisms of NF-κB activation induced by bacterial lipopolysaccharide through Toll-like receptors," *Journal of Endotoxin Research*, vol. 6, no. 6, pp. 453–457, 2000.

[16] M. Triantafilou and K. Triantafilou, "The dynamics of LPS recognition: complex orchestration of multiple receptors," *Journal of Endotoxin Research*, vol. 11, no. 1, pp. 5–11, 2005.

[17] S.-H. Eom, S.-H. Lee, N.-Y. Yoon et al., "α-Glucosidase- and α-amylase-inhibitory activities of phlorotannins from *Eisenia bicyclis*," *Journal of the Science of Food and Agriculture*, vol. 92, no. 10, pp. 2084–2090, 2012.

[18] M. B. Hansen, S. E. Nielsen, and K. Berg, "Re-examination and further development of a precise and rapid dye method for measuring cell growth/cell kill," *Journal of Immunological Methods*, vol. 119, no. 2, pp. 203–210, 1989.

[19] B. Xue, Y. Wu, Z. Yin et al., "Regulation of lipopolysaccharide-induced inflammatory response by glutathione S-transferase P1 in RAW264.7 cells," *FEBS Letters*, vol. 579, no. 19, pp. 4081–4087, 2005.

[20] N. Rajapakse, M.-M. Kim, E. Mendis, and S.-K. Kim, "Inhibition of inducible nitric oxide synthase and cyclooxygenase-2

in lipopolysaccharide-stimulated RAW264.7 cells by carboxybutyrylated glucosamine takes place via down-regulation of mitogen-activated protein kinase-mediated nuclear factor-κB signaling," *Immunology*, vol. 123, no. 3, pp. 348–357, 2008.

[21] D. Le Huu, T. Matsushita, G. Jin et al., "IL-6 blockade attenuates the development of murine sclerodermatous chronic graft-versus-host disease," *Journal of Investigative Dermatology*, vol. 132, no. 12, pp. 2752–2761, 2012.

[22] W.-K. Jung, D.-Y. Lee, C. Park et al., "Cilostazol is anti-inflammatory in BV2 microglial cells by inactivating nuclear factor-kappaB and inhibiting mitogen-activated protein kinases," *British Journal of Pharmacology*, vol. 159, no. 6, pp. 1274–1285, 2010.

[23] H. J. Kang, S. H. Hong, K.-H. Kang, C. Park, and Y. H. Choi, "Anti-inflammatory effects of Hwang-Heuk-San, a traditional Korean herbal formulation, on lipopolysaccharide-stimulated murine macrophages," *BMC Complementary and Alternative Medicine*, vol. 15, article 447, 2015.

[24] S. W. A. Himaya, B. Ryu, Z.-J. Qian, and S.-K. Kim, "Paeonol from *Hippocampus kuda* Bleeler suppressed the neuro-inflammatory responses in vitro via NF-κB and MAPK signaling pathways," *Toxicology in Vitro*, vol. 26, no. 6, pp. 878–887, 2012.

[25] Y. Pan, Y. Wang, L. Cai et al., "Inhibition of high glucose-induced inflammatory response and macrophage infiltration by a novel curcumin derivative prevents renal injury in diabetic rats," *British Journal of Pharmacology*, vol. 166, no. 3, pp. 1169–1182, 2012.

[26] C. Zhang, Y. Li, Z.-J. Qian, S.-H. Lee, Y.-X. Li, and S.-K. Kim, "Dieckol from Ecklonia cava regulates invasion of human fibrosarcoma cells and modulates mmp-2 and mmp-9 expression via NF-b pathway," *Evidence-Based Complementary and Alternative Medicine*, vol. 2011, Article ID 140462, 8 pages, 2011.

[27] W.-K. Jung, Y.-W. Ahn, S.-H. Lee et al., "*Ecklonia cava* ethanolic extracts inhibit lipopolysaccharide-induced cyclooxygenase-2 and inducible nitric oxide synthase expression in BV2 microglia via the MAP kinase and NF-κB pathways," *Food and Chemical Toxicology*, vol. 47, no. 2, pp. 410–417, 2009.

[28] Y. Lee, W.-J. Sohn, D.-S. Kim, and H.-J. Kwon, "NF-κB- and c-Jun-dependent regulation of human cytomegalovirus immediate-early gene enhancer/promoter in response to lipopolysaccharide and bacterial CpG-oligodeoxynucleotides in macrophage cell line RAW 264.7," *European Journal of Biochemistry*, vol. 271, no. 6, pp. 1094–1105, 2004.

[29] J. Wang and G. Mazza, "Inhibitory effects of anthocyanins and other phenolic compounds on nitric oxide production in LPS/IFN-γ-activated RAW 264.7 macrophages," *Journal of Agricultural and Food Chemistry*, vol. 50, no. 4, pp. 850–857, 2002.

[30] A.-R. Kim, T.-S. Shin, M.-S. Lee et al., "Isolation and identification of phlorotannins from *Ecklonia stolonifera* with antioxidant and anti-inflammatory properties," *Journal of Agricultural and Food Chemistry*, vol. 57, no. 9, pp. 3483–3489, 2009.

[31] D.-O. Moon, Y. H. Choi, N.-D. Kim, Y.-M. Park, and G.-Y. Kim, "Anti-inflammatory effects of β-lapachone in lipopolysaccharide-stimulated BV2 microglia," *International Immunopharmacology*, vol. 7, no. 4, pp. 506–514, 2007.

[32] C. J. Hawkey and M. J. S. Langman, "Non-steroidal anti-inflammatory drugs: overall risks and management. Complementary roles for COX-2 inhibitors and proton pump inhibitors," *Gut*, vol. 52, no. 4, pp. 600–608, 2003.

[33] Y. Sugiura, R. Tanaka, H. Katsuzaki, K. Imai, and T. Matsushita, "The anti-inflammatory effects of phlorotannins from *Eisenia arborea* on mouse ear edema by inflammatory inducers," *Journal of Functional Foods*, vol. 5, no. 4, pp. 2019–2023, 2013.

[34] Y. Fujii, R. Tanaka, H. Miyake, Y. Tamaru, M. Ueda, and T. Shibata, "Evaluation for antioxidative properties of phlorotannins isolated from the brown alga *Eisenia bicyclis*, by the H-ORAC method," *Food and Nutrition Sciences*, vol. 4, no. 8, pp. 78–82, 2013.

[35] N. Y. Yoon, S.-H. Lee, K. B. Shim et al., "Quinone reductase induction activity of phlorotannins derived from *Eisenia bicyclis* in Hepa1c1c7 cells," *Fisheries and Aquatic Science*, vol. 16, no. 1, pp. 1–5, 2013.